Wave-mixing with high-order harmonics in extreme ultraviolet region

Lap Van Dao, Khuong Ba Dinh, Hoang Vu Le, Naylyn Gaffney, and Peter Hannaford

Citation: Applied Physics Letters **106**, 021118 (2015); doi: 10.1063/1.4906120
View online: http://dx.doi.org/10.1063/1.4906120
View Table of Contents: http://scitation.aip.org/content/aip/journal/apl/106/2?ver=pdfcov
Published by the AIP Publishing

Wave-mixing with high-order harmonics in extreme ultraviolet region

Lap Van Dao, Khuong Ba Dinh, Hoang Vu Le, Naylyn Gaffney, and Peter Hannaford
Centre for Quantum and Optical Science, Swinburne University of Technology, Melbourne 3122, Australia

(Received 16 November 2014; accepted 6 January 2015; published online 15 January 2015)

We report studies of the wave-mixing process in the extreme ultraviolet region with two near-infrared driving and controlling pulses with incommensurate frequencies (at 1400 nm and 800 nm). A non-collinear scheme for the two beams is used in order to spatially separate and to characterise the properties of the high-order wave-mixing field. We show that the extreme ultraviolet frequency mixing can be treated by perturbative, very high-order nonlinear optics; the modification of the wave-packet of the free electron needs to be considered in this process. © *2015 AIP Publishing LLC*. [http://dx.doi.org/10.1063/1.4906120]

When atoms or molecules interact with an intense laser field, high-order harmonics generation (HHG) of the incident radiation may be generated. This process provides methods to produce short pulses of coherent radiation in the extreme ultraviolet (XUV) and soft x-ray region. Such an HHG source opens up new applications such as in time-resolved studies of atoms[1] and molecules,[2] extreme ultraviolet interferometry,[3] and coherent diffractive imaging.[4] From the point of view of fundamental research, high-order harmonic generation is an example of nonlinear physics, where simple pictures can be used to describe strongly non-perturbative processes with the time-dependent Schroedinger equation. This highly nonlinear process leading to the up-conversion of low energy photons into XUV or x-ray photons can be conceptually understood classically in the so-called three-step model[5] in which an electron is first liberated from an atom through strong field ionization, then is accelerated by the laser field, and finally is recombined with the parent ion, emitting any excess energy as a high-energy photon.

When matter interacts with a laser field, the response of the medium described by the polarization term can be expanded in many orders,[6] expressed as linear and nonlinear terms. Depending on the strength of the field, the highest orders of response need to be considered. The low-order response of a material to a laser field, e.g., third or fifth order, has been used to study structures of matter and their dynamics.[7] Several nonlinear phenomena appear in the regime of extreme interactions. The detailed response of a single atom or molecule to an intense electromagnetic field is quite complex, but the fundamental underlying physics can be unexpectedly simple in many cases. Bertrand *et al.*[8] have shown that when two intense fundamental laser pulses of frequency ω and 2ω are crossed non-collinearly in a gas-jet target, the emission spectrum can be described simply in terms of conservation of energy and momentum based on the net number of photons absorbed from each laser field. The observation of nonlinear optical wave-mixing in HHG[8] also suggests the possibility to treat the physics in the XUV range with a *perturbative* nonlinear optics theory although perturbative and *nonperturbative* nonlinear optics seem conceptually very different. Because in the far-field long and short trajectories of HHG processes are spatially separated and because the off-axis emission results in an annular beam and even-order harmonics can be generated by combination of ω, 2ω fields,[9] the use of incommensurate frequency fields allows the generation of non-integer order harmonics which are spatial separated. The non-integer order harmonics provide more clear characterization of wave-mixing.

In this paper, we report the investigation of the wave-mixing process with two long (40 fs) pulses with incommensurate frequencies (at 1400 nm and 800 nm). Using a non-collinear scheme for the two beams, which helps to spatially separate the extreme ultraviolet field according to the mixing condition, we study the properties of the high-order frequency mixing field. We show that a treatment of the free electrons needs to be considered in the wave-mixing process and perturbative nonlinear optics can be observed in a high-order nonlinearity.

A 800 nm, 9 mJ, 30 fs, 1 kHz repetition rate laser beam is split into two beams, with pulse energies of 6 mJ and 3 mJ. The 6 mJ beam is used to pump a three-stage optical parametric amplifier (OPA) system to generate an infrared (IR) driving pulse at 1400 nm with energy of ~2 mJ and duration of 40 fs. One path (~1 mJ) of the 3 mJ, 800 nm beam is used to mix with the 1400 nm field. The 1400 nm IR pulse is used for phase-matched generation of XUV pulses and the 800 nm pulse, which is used to control the HHG output, is aligned at a very small angle ($<1°$) to the direction of the 1400 nm beam by a dichroic mirror. The intensity of the 800 nm pulse is kept low so that high-order harmonics cannot be generated by itself. The polarizations of the two pulses are parallel. The time delay between the two pulses is controlled by a motorized delay stage with 0.1 fs resolution. The laser beams are used to drill a pinhole in a thin aluminium plate at the end of the cell for the output of the HHG field and no further alignment procedure along the optical axis of the 1400 nm pulse is needed. The diameter of the two beams at the focus is ~100 μm. A long (~30 mm) cell filled with argon gas at a pressure of ~250 Torr is used as the interaction medium.[10,11] The interaction length where the XUV radiation is generated is ~1 mm before the end of the cell. Positive time delay implies that the 800 nm pulse precedes the 1400 nm pulse. A non-collinear scheme of the two beams helps to spatially separate the wave-mixing field from the 1400 nm and 800 nm beams because of momentum conservation. The harmonic emission enters a flat-field XUV

spectrometer comprising a slit, a concave grating, and a cooled 14-bit CCD camera. The length of the slit is along the Y direction and therefore the divergence can be determined along the Y direction of the CCD. The harmonic emission is dispersed along the X direction of the CCD.

Figure 1 shows the spatially integrated HHG spectrum versus delay time between the 1400 nm and 800 nm pulses in the far-field. The high-order harmonic radiation is generated at wavelengths down to 16 nm when the 1400 nm driving pulse is applied. When the 800 nm pulse is absent or for very long delay times ($>\pm 200$ fs), we obtain phase-matched radiation[12] with well-resolved odd harmonics and a good beam profile along the propagation direction of the 1400 nm driving pulse. The spectrum of the XUV radiation varies markedly with the influence of the second pulse. At zero delay between the two pulses, a quasi-continuum XUV spectrum is obtained (Fig. 1). The addition of the second optical field whose frequency is not commensurate with that of the primary field creates additional frequency components in the HHG spectrum.

The spectrum and spatial features, which are observed on the CCD, are modified with the delay time between the two pulses. For long delay time (>200 fs), a Gaussian beam profile along the axis of the driving pulse is obtained, while for short delay times the beam profile consists of many clearly resolved peaks. In Fig. 2, we show the spectrum versus divergence from the 1400 nm beam direction for a fixed time delay ~10 fs, as an example. The discrete spatial and spectral peaks in the CCD image are caused by frequency mixing of the two fields—the harmonic field generated by the 1400 nm driving beam and the delayed 800 nm controlling field. The spectrum exhibits distinct peaks in the low photon energy region (<50 eV), while there are no clear peaks at high photon energy. This may be because the spectrometer resolution is not high enough in the high-photon energy region. The spatial and spectral positions of the peaks vary with delay time between the two pulses as shown in the inset of Fig. 2. The spectral and spatial separation of the peaks is likely to be unchanged for a given delay. The 1400 nm beam alone generates a high-harmonic spectrum along the optical axis (divergence $\theta = 0$ as shown in the inset of Fig. 1). The addition of the weak 800 nm field gives rise to off-axis

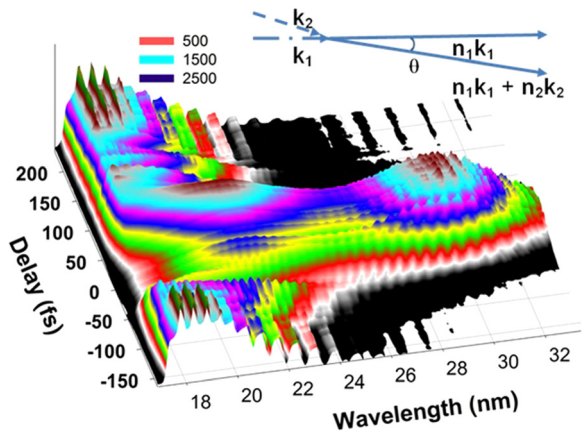

FIG. 1. Spatially integrated HHG spectrum generated by a 1400 nm driving pulse versus delay time of the 800 nm controlling pulse. The inset shows the propagation direction of the fields.

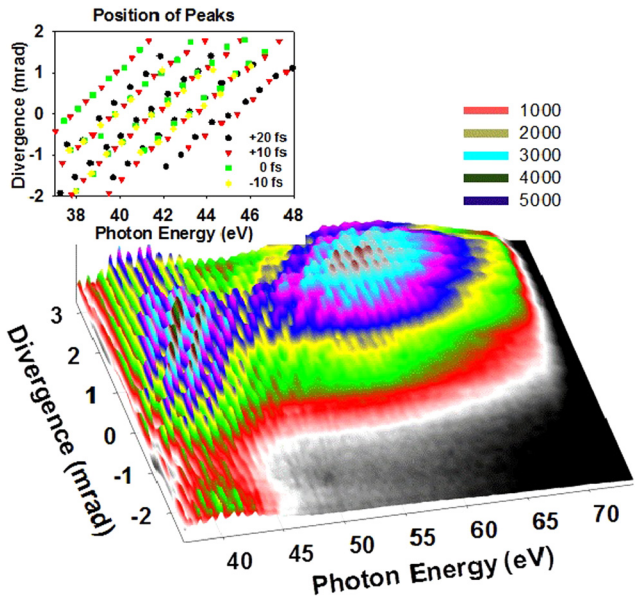

FIG. 2. HHG spectrum versus angular divergence for the focus plane of the spectrometer at a delay time of ~10 fs between the 1400 nm and 800 nm pulses. The inset shows the spatial and spectral position of the peaks at different delay times between the 1400 nm and 800 nm pulses.

radiation at different angles in the vertical Y direction. Conservation of energy and momentum for the generation of the resulting XUV emission needs to be considered.

To emit a single XUV photon, parity conservation requires that for a dipole transition the wave function of the continuum electron and the ion together must be in a state of different parity to that of the original ground state.[13] Therefore, only the net absorption of an odd total number of photons $n = n_1 + n_2$ can lead to photon emission, where n_1 and n_2 are the number of photons with frequency ω_1 and ω_2. Because the second field is weak, $n_1 \gg n_2$. These selection rules can be written alternatively as: $\omega_q = n_1\omega_1 + n_2\omega_2$; $\mathbf{k_q} = n_1\mathbf{k_1} + n_2\mathbf{k_2}$; and $n_1 + n_2 = 2j + 1$, where j is an integer, ω_1 is the carrier frequency of the 1400 nm field, and ω_2 is the carrier frequency of the 800 nm field. From this approach, it is possible to produce a radiated frequency $\omega_q = (2j+1)\omega_1 \pm n(\omega_2 - \omega_1)$ along directions $\mathbf{k_q} = (2j+1)\mathbf{k_1} \pm n(\mathbf{k_2} - \mathbf{k_1})$ for various (j, n) combinations. The harmonic number j is determined by the spectrum generated by the 1400 nm beam only. The energy difference between neighbouring peaks is ~0.67 eV, which is consistent with 800 nm and 1400 nm fields. The addition or subtraction of photons is reflected in the position of the additional frequency components along the Y axis. The spectral and spatial positions of the mixing peaks vary with delay time between the two beams which indicate $\omega_q = (2j+1)\omega_1 \pm n(\omega_2 - \omega_1) + \delta\omega$ and the directions $\mathbf{k_q} = (2j+1)\mathbf{k_1} \pm n(\mathbf{k_2} - \mathbf{k_1}) + \delta\mathbf{k}$, where $\delta\omega$ and $\delta\mathbf{k}$ are dependent on the phase of the interaction of the 800 nm field. The effect of plasma dispersion on the propagation of the visible and near-infrared fields causes phase effects in the propagation of the 800 and 1400 nm fields. With the presence of free electrons due to ionization, the wave number of these fields is shifted to $k_1^2 = k_0^2(1 - \omega_p^2/\omega_0^2)$, where $\omega_P = e\sqrt{\frac{N_e}{\varepsilon_0 m_e}}$ is the plasma frequency, N_e is the density of free electrons, ε_0 is the vacuum permittivity, m_e is the electron

mass, and ω_0 and k_0 are the frequency and wave-vector of the laser field, respectively.

We assume that the high-order harmonics are weakly perturbed by propagation in the medium because of atomic and plasma dispersion. The atomic dipole phase, acquired by the electron wave function in the continuum due to the delay between the ionization and recombination times, is not negligible. This phase needs to be considered in the harmonic field and scales linearly with the driving laser intensity, $\Phi_q(r,z) = -\alpha_q I(r,z)$, where α_q is a coefficient related to the electron trajectories: $\alpha_q \approx 1 - 5 \times 10^{-14}\,\mathrm{cm}^2/\mathrm{W}$ for a short trajectory and $\alpha_q \approx 20 - 25 \times 10^{-14}\,\mathrm{cm}^2/\mathrm{W}$ for a long trajectory,[14] where r is the radial coordinate and z is along the propagation direction. The momentum of the harmonic photon is the sum of the momenta of the incident laser photons and the excess momentum provided to the laser beam by the free electron which is $\delta \boldsymbol{k_q} = \nabla \Phi_q(r, z)$. It can be shown[15] that $\delta \boldsymbol{k_q}$ can be interpreted as the canonical momentum gained by the free electron in the second step of the three-step model, as a result of the ponderomotive force. The ponderomotive force effects are essential to ensure momentum conservation of the coupled atom-laser and harmonic field system. When two fields with incommensurate frequencies are summed, the total electric field is significantly different from that of a simple sinusoidal field and the electron trajectories are strongly dependent on the given optical cycle. This situation may open a dynamical regime of frequency mixing.

When two pulses are delayed in time, the variation of HHG intensity reflects the dependence of the harmonic field on the intensity of the second field. The 800 nm field modifies the trajectory of the free electron created by the 1400 nm field which leads to the generation of additional energy and momentum of the mixing field that is reflected in a shift of the peak along the divergence direction as shown in the inset of Fig. 2.

The dependence of the dipole phase on the intensity of the laser fields affects not only the total phase but also the spectrum of the emitted fields. The variation in time of the fundamental laser intensity, I(t), induces a change in the instantaneous frequency of the harmonic emission through a harmonic phase modulation process.[16,17] The instantaneous harmonic frequency during the pulse is given by[15]

$$\omega_q(t) = q\omega + \alpha_q \frac{\partial I}{\partial t}. \tag{1}$$

Here, $q\omega$ is the central harmonic frequency and the term $\alpha_q \frac{\partial I}{\partial t}$ gives the variation of the instantaneous frequency with time. From Eq. (1), the spectral broadening is given by

$$\delta\omega_q(t) = \alpha_q \frac{\partial I}{\partial t}. \tag{2}$$

From Eq. (2), since a long path with a large coefficient α_q is predominantly phase-matched off-axis, the off-axis region would give a larger shifting and broadening than the on-axis region.

For negative delay times, the spectrum bandwidth of the harmonic field increases with decreasing delay time and the spectrum position is slightly shifted. With increasing positive delay time, a large spectral shift is observed. Figure 3 shows a detailed study of the spectral position of the peaks when the divergence is kept constant around the harmonics H47 and H49. We note that for easy analysis of the spectral shift, the divergence for the same j and n values is kept constant. The results of Fig. 3 can be interpreted in the following way: for negative delay times, $\tau \leq 0$ fs, when the 800 nm pulse interacts mostly with an atom in the ground state, the spectral position of the peak is nearly unchanged because of weak modification of the dipole phase. For positive delay times, the interaction of the 800 nm field with a free electron created by the 1400 nm pulse is very strong since the free electron trajectory can be easily modified and also the 800 nm beam crosses the interaction region. In this case, additional excess energy can be provided to the free electron and the spectral position is shifted.

For negative time delay, the intensity of different frequency components, which are assigned the same value of j and a different value of n, increases at different rates and then saturates. For delay times ≤ 0, the intensity of the wave-mixing signal grows linearly with the intensity of the 800 nm field when $n \leq 0$, where $n = 0$ is for the peak at $\theta \approx 0$. The slope increases with increasing n for $n > 1$. This is similar to the observation of Bertrand *et al.*[8] when the intensity of the second field is increasing. The wave-mixing radiation decreases rapidly for positive delay times because of the modification of the free electron trajectory by the weak 800 nm field. The generation of high-order harmonics caused by the high intensity 1400 nm driving field is a nonperturbative process but it can be treated perturbatively for the mixing process with a weaker 800 nm second field and for the case in which only atoms in the ground state are considered.

It is well known that the XUV HHG spectra show strong modulation involving the interference of harmonics which is dependent on the harmonic photon energy and is not caused by absorption in the generating medium. The single-atom response and also collective effects through the phase-mismatch are probably involved in determining these spectral features, but separation of the influence of phase matching on the harmonic yield is not easily identifiable. In our wave-mixing experiment (Fig. 1), a minimum in the spectrum can be seen at ~51 eV (24 nm) where a Cooper

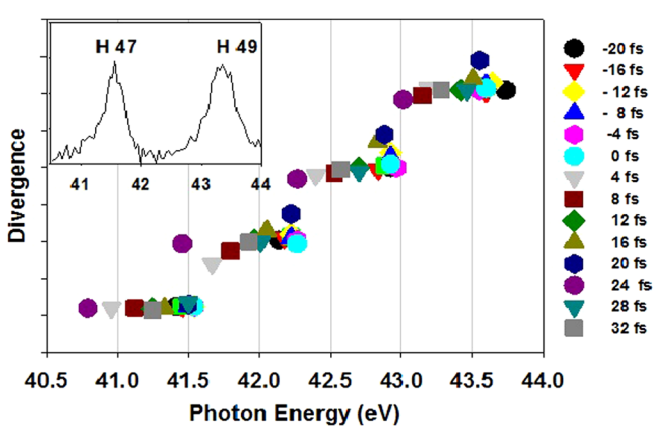

FIG. 3. Spectrum position of the wave-mixing peaks at different delay times between the 1400 nm and 800 nm pulses around the 47th and 49th harmonics.

minimum caused by destructive interference of the 5s and 4d transition dipole moments is expected.[18,19] The appearance of the minimum is independent of the experimental parameters such as the angle between the two beams and their intensity ratio. The observation of a Cooper minimum in the mixing spectrum indicates that a combination of single-atom responses in the nonlinear atomic dipole moment can be used in a theoretical treatment. The different dipole phase of the two regions, of higher and lower energy, around the minimum causes the different development of the mixing spectrum versus time delay.

In conclusion, the combination of two fields with controllable intensity ratio opens a way for the generation of additional frequency components which is a step towards obtaining attosecond pulses with high intensity in the soft x-ray region. A perturbative treatment in the high-order harmonic frequency region will help in the investigation of quantum effects in atoms and molecules in the high photon energy range.

[1]M. Uiberacker, M. Schultze, A. J. Verhoef, V. Yakovlev, M. F. Kling, J. Rauschenberger, N. M. Kabachnik, H. Schröder, M. Lezius, K. L. Kompa *et al.*, Nature **446**, 627 (2007).
[2]E. Gagnon, P. Ranitovic, X. M. Tong, C. L. Cocke, M. M. Murnane, H. C. Kapteyn, and A. S. Sandhu, Science **317**, 1374 (2007).
[3]D. Descamps, C. Lynga, J. Norin, A. L'Huillier, C. G. Wahlström, J. F. Hergott, H. Merdji, P. Salières, M. Bellini, and T. W. Hänsch, Opt. Lett. **25**, 135 (2000).
[4]B. Chen, R. A. Dilanian, S. Teichmann, B. Abbey, A. G. Peele, G. J. Williams, P. Hannaford, L. V. Dao, H. M. Quiney, and K. A. Nugent, Phys. Rev. A **79**, 023809 (2009).
[5]P. B. Corkum, Phys. Rev. Lett. **71**, 1994 (1993).
[6]N. Bloembergen and P. S. Pershan, Phys. Rev. **128**, 606–622 (1962).
[7]S. Mukamel, *Principles of Nonlinear Optical Spectroscopy* (Oxford University Press, 1995).
[8]J. B. Bertrand, H. J. Woerner, H. C. Bandulet, E. Bisson, M. Spanner, J. C. Kieffer, D. M. Villeneuve, and P. B. Corkum, Phys. Rev. Lett. **106**, 023001(4) (2011).
[9]I. J. Kim, H. T. Kim, C. M. Kim, J. J. Park, Y. S. Lee, K. H. Hong, and C. H. Nam, Appl. Phys. B: Lasers Opt. **78**, 859–861 (2004).
[10]S. Teichmann, P. Hannaford, and L. V. Dao, Appl. Phys. Lett. **94**, 171111 (2009).
[11]L. V. Dao, H. Chris, H. L. Vu, K. B. Dinh, E. Balaur, P. Hannaford, and T. Smith, Appl. Opt. **51**, 4240 (2012).
[12]T. Popmintchev, M. C. Chen, O. Cohen, M. E. Grisham, J. J. Rocca, M. M. Murnane, and H. C. Kapteyn, Opt. Lett. **33**, 2128–2130 (2008).
[13]A. Fleischer and N. Moiseyev, Phys. Rev. A **74**, 053806 (2006).
[14]T. Auguste, P. Salières, A. S. Wyatt, A. Monmayrant, I. A. Walmsley, E. Cormier, A. Zaïr, M. Holler, A. Guandalini, F. Schapper, J. Biegert, L. Gallmann, and U. Keller, Phys. Rev. A **80**, 033817 (2009).
[15]P. Balcou, P. Salieres, A. L'Huillier, and M. Lewenstein, Phys. Rev. A **55**, 3204 (1997).
[16]C. Kan, C. E. Capjack, R. Rankin, and N. H. Burnett, Phys. Rev. A **52**, R4336 (1995).
[17]C. M. Hey, J. Güdde, U. Höfer, and A. L'Huillier, Phys. Rev. Lett. **107**, 033903 (2011).
[18]H. J. Worner, H. Niikura, J. B. Bertrand, P. B. Corkum, and D. M. Villeneuve, Phys. Rev. Lett. **102**, 103901(4) (2009).
[19]K. B. Dinh, H. V. Le, P. Hannaford, and L. V. Dao, J. Appl. Phys. **115**, 203103 (2014).